FUNDAMENTAL STUDY ON DYNAMIC BEHAVIOUR OF MULTI-STORY SHEAR WALLS

T. Shimazu (I)
H. Araki (II)
Presenting Author: H. Araki

SUMMARY

This paper presents shaking table tests conducted with an aim to establish the method of evaluating earthquake resistance of multi-story shear walls. The variables considered are the number of stories, the support condition of wall bases and earthquake motion inputs. The number of test structures totaled fourty-four.

The relations among the variables, the transitions of periods and modes along input levels, interstory shear and displacement loop hysteresis and maximum lateral distribution shapes along height at each input level on both the load and deflection are discussed.

INTRODUCTION

It has been recognized from many experiences of earthquake building damages that shear walls are the most effective elements in securing the structural safety of buildings against earthquake motions, also from the view point of controlling the lateral deflections. There have been numerous studies on shear walls. However, the majority of these studies are based on static loading (Ref. 1), not dynamic loading corresponding with the response to earthquake motions. Very recently several researches (Ref. 2,3) using shaking table have been performed with emphasis on the time history characteristics of structure response to earthquake motions. However, what seems to be more important is to develope the simplified method for evaluating both the maximum lateral force and deflection distributions induced in buildings against any level of earthquake motion for the rational earthquake resistant design of shear walls.

TEST PROGRAM

Test structures are about one- fifteen scale shear wall-frame structures as shown in Fig. 1. Fourty-four structures were tested in total as shown in Table 1. The main variable was the number of stories and the others were the arrangement of reinforcement in walls, base support conditions as well as the type of base motion inputs. Two types of base motion inputs were given. One is the scaled recorded earthquake acceleration motions for thirty-four test structures while the other is sinu-

---

(I) Assoc. Prof. ,Faculty of Engineering, University of Hiroshima Japan

(II) Research Associate, Faculty of Engineering, University of Hiroshima Japan

soidal base motions for the remaining ten structures. However, the focus is placed on the tests of scaled recorded earthquake motions (1940 El Centro EW and 1952 Taft S69E) as such test results were assumed to give a direct information for the rational design of shear walls. Structures were tested using the Earthquake Simulator of the Chugoku- Electric Com. Ltd. A test structure was bolted to the platform and then masses were connected. The stability in the direction perpendicular to the input motion was provided at the top of test structure with a set of rollers whose friction force can be assumed negligible, as shown in Fig. 2. The time scale 1/4 was used for the inputs of the recorded earthquake motions, taking into account the scale effects for test structures. The response velocity spectra on the recorded earthquake motions can basically be modeled into bilinear curves (Ref. 4) as shown Fig. 3. In order to apply directly the test results for actual structures, factor k (=T/To) was defined as the ratio of initial fundamental period T of structure to the transition point period To which was determined as To=0.04 sec for the response velocity spectra in Fig. 3. The thirty-four test structures were subjected to the desired earthquake base motion at the specified acceleration levels of each Run with small amplitude free vibration tests inserted before every Run starts in order to obtain the changed natural periods while the remaining ten structures were subjected to sinusoidal base motion of each Run with small amplitude tests inserted. The acceleration and displacement time histories at several stories were measured with sensors attached to highly stiffened steel frame constructed on the platform of the shaking table. The test structures were cast horizontally out of the same batch of concrete. The material properties of both the concrete and steel used are shown in Table 2.

TEST RESULTS

Crack patterns up to failure stage are illustrated in Fig. 4. Shear cracks are found for almost all the test structures besides those (B8 E, B8 T) in which shear walls are supported by foundation beams. Final failure occured by flexure at the bottom end of shear walls for almost all the structures except the above structures (B8 E, B8 T) and pierced shear wall structures (08 E, 04 E).

Hysteresis loops are also illustrated for each Run in Fig. 5. It is seen that the phase is consistent between base shear and displacement for the four-story structure while the phase lags exists between them for eight-story or sixteen-story structures in which the second modes seem to be predominant. Fig. 6-a and 6-b illustrated both the maximum lateral force and deflection distributions observed.

DISCUSSIONS

In the following, fundamental periods and their transitions, ultimate strength, maximum lateral load and deflection distributions along with input levels will be discussed.

Fundamental Periods and Their Transitions after Each Run

Fig. 7 shows the test values of initial fundamental periods for all the fourty-four structures at the first stage of Run 1 with calculated

values that were obtained by using the three moment equation (Ref. 5) for wall-frame systems. For pierced shear wall type, calculated values were obtained by generalized D values Method. It is found that there is good agreement between test and calculated values for both the types of structures. Fig. 8 shows the extents of fundamental periods and equivalent damping ratios along with Run levels. These values were obtained from small amplitude free vibration test done after each Run. It is seen that fundamental periods increase 1.3~2.0 times, depending upon the number of stories, and that equivalent damping ratios also increase remarkably with Run levels.

Ultimate Strength

Fig. 9 shows maximum base shear observed (at Run 4). The plus and minus values are nearly the same for all the structures. Calculated values were obtained for three assumed types of lateral load distributions, inverted triangular, uniform and triangular. Each value was obtained by assuming the collapse mechanism with the method of virtual work. Varying axial load effects were taken into account for column strength. The method for obtaining cross sectional flexural and shear strength are as follows. The shape of cross section in walls is not rectangular but was assumed to be equivalent rectangular one having the same gross area for calculating flexural or shear strength. The center of compression block is assumed to be one of the outermost column with all the reinforcement yielding in tension even for pierced shear walls in which the effect of reinforcement is excluded for opening area. It is seen from Fig. 9 that maximum base shears for four-story, eight-story and sixteen-story center core structure are consistent with those of ultimate strengths calculated for inverted triangular, uniform and triangular lateral force distributions respectively, with coupled shear wall or pierced shear walls showing a little shifted trends.

Lateral Force Distribution as well as Maximum Base Shear Values along with Run Level

Fig. 10 shows the relations between the maximum base shear and response velocity S_{VA}, obtained by dividing spectral intensity (Ref. 6) with corresponding period range T_{range} (0.025~0.625 sec), along with Run level. Base shear values increase nearly linearly with average response velocity at first stage, butgradually lie down, approaching maximum point. The line shown in Fig. 10 was obtained by assuming the test structure as single-degree-of-freedom system having fundamental period explained in the previous section, subjected to the impulse whose value is average response velocity S_{VA} as follows.

$$\text{Base shear} = \frac{2\pi}{T} \frac{W}{g} S_{VA} \qquad (1\text{-a})$$

$$S_{VA} = \frac{I_{002}}{T_{range}} \qquad (1\text{-b})$$

Fig. 11 shows an equation obtained by normalizing these curves for test structures in Fig. 10.

$$\eta = f(\xi) = 1.7\xi^3 - 4.0\xi^2 + 3.3\xi \qquad (2)$$

Fig. 12 shows the amplification factor r to calculated ultimate strength Puo obtained by assuming inverted triangular lateral force distributions.

$$Pu = Puo \cdot r \qquad (3\text{-a})$$

$$r = 0.78 \cdot k^{0.63} \qquad (3\text{-b})$$

Using above equations yields the following

$$\text{Base shear} = Puo \cdot r \cdot f\left(\frac{S_{VA}}{S_{VA\,max}}\right) \qquad (4\text{-a})$$

$$S_{VA\,max} = \frac{Puo \cdot r}{\left(\frac{W_T}{g}\frac{2\pi}{T}\right)} f'(0) = 3.3\,\frac{Puo \cdot r}{\left(\frac{W_T}{g}\frac{2\pi}{T}\right)} \qquad (4\text{-b})$$

Fig. 13 shows the comparison between the test and calculated values. There is good agreement between them. Fig. 14 shows the ratios of top to third floor maximum accelerations observed at each Run level, with a curve obtained from Eq. (3-b). It is seen that observed acceleration values are basically consistent with those by r values. Thus the shape of lateral force distributions which give maximum base shear was ascertained to vary remarkably with fundamental period factor k values. However, the situation is quite different for maximum overturning moment. Fig. 15 shows the comparison between test and calculated values on maximum overturning moment. There is good agreement. The calculated values were obtained by distributing the above maximum base shear in inverted triangular shape, regardless of k values.

Lateral Displacement Distribution along with Run Level

Fig. 16 shows the comparison between test and calculated values on deformation angle at the height of 2/3·H in which H is total height of structure. Calculated values were obtained as follows, using the single-degree-of-freedom system as explained above,

$$R = \frac{T}{2\pi} \cdot \frac{S_{VA}}{2/3 \cdot H} \qquad (5)$$

It is seen that there is basically good agreement between both the values. Fig. 16 shows the comparison between relative deformation angles.

Comparison with Lateral Force Distributions Obtained from the Design Story Shear Coefficient Prescribed in Recently Revised Code of Japan

Fig. 18 shows the comparison between lateral force distribution obtained from Eq. (3-b) in tests and that calculated from the code for the sixteen-story test structures. It is seen that the difference is remarkable. The design story coefficient given in the code seems to be mainly due to the maximum values obtained separately at each level without taking into account

the fact that those values never occur simultaneously. The code curves are the envelope of maximum values at each floor, which are similar to those by modal analysis. It can be said that the code values are too conservative for high rise buildings.

CONCLUSIONS

Based on the experimental works which deal with walls of uniform cross section along height, as a basic step which is also the most important, the following conclusions can be made.

1. Fundamental periods in the range of small amplitudes can be estimated by the elastic theory at initial stage, but increase gradually up to 1.3 2.0 times at failure stage with earthquake input level, depending upon the values of initial periods.
2. Equations are proposed for both the maximum lateral force and displacement distributions induced by earthquake motions, based on the simple theoretical model as well as the estimated values of ultimate strength.
3. Finally, comparisons were made between test results and those by recently revised code of Japan.

REFERENCES

1. M. Hirosawa,"Past Experimental Results on Reinforced Concrete Shear Walls and Analysis on Them," (in Japanese) Kenchiku Kenkyu Shiryo No.6 March 1975
2. M.A. Sozen and D.P.Abram, "Experimental Study of Frame-Wall Interaction in Reinforced Concrete Structures Subjected to Strong Earthquake Motions", Civil Engineering Studies, SRS No.460, University of Illinois, Urbana-Champaign, May 1979
3. S. Otani, "Earthquake Tests of Shear Wall Frame Structure," Sixth World Conference Earthquake Engineering 1977
4. N.M. Newmark and R.Riddell,"Inelastic Spectra for Seismic Design," Seventh World Conference Earthquake Engineering 1980
5. Y. Osawa and T. Koh, "A Proposal of the Structural Analysis of Core-Wall Buildings Subjected to Lateral Forces - Elastic and Elasto-Plastic Analysis," Transactions of the Architectural Insititute of Japan, No101, August 1964
6. G.W. Housner, "Behaviour of Structures during Earthquakes," Journal of Engineering Mechanics Division, ASCE, EM4 1959

Table 1 List of Test Structures

Story	Type	Test Structure	Base Motion	Remarks
4	Center Core Structure	C4 E	1940 El Centro EW	
		C4 T	1952 Taft S69E	
		C4 1st	Sin Wave 1st Mode	
		C4 E once	1940 El Centro EW	
		C4 E	"	
	Isolated Wall	IS4 E	"	
		IS4 T	1952 Taft S69E	
		IS4 1st	Sin Wave 1st Mode	
	Center Core Structure	C4 E pt	1940 El Centro EW	pt*2 normal pt
		C4 E pw	"	pw*1/4 normal pw
		B4 E	"	Foundation Girder
	Eccentric Wall	E4 E	"	
	Pierced Wall	O4 E	"	
8	Center Core Structure	C8 E	"	
		C8 T	1952 Taft S69E	
		C8 1st	Sin Wave 1st Mode	
		C8 2nd	Sin Wave 2nd Mode	
		C8 E once	1940 El Centro EW	
		C8 E 1/8	"	1/8 Time Scale
	Isolated Wall	IS8 E	"	
		IS8 T	1952 Taft S69E	
		IS8 1st	Sin Wave 1st Mode	
		IS8 2nd	Sin Wave 2nd Mode	
	Center Core Structure	C8 E pt	1940 El Centro EW	pt*2 normal pt
		C8 E pw	"	pw*1/4 normal pw
		B8 E	"	Foundation Girder
		B8 T	1952 Taft S69E	"
		C8-1 E	1940 El Centro EW	Beam Type
	Eccentric Wall	E8 E	"	
	Coupled Wall	C8-2 E	"	
	Pierced Wall	O8 E	"	
16	Center Core Structure	C16 E	"	
		C16 T	1952 Taft S69E	
		C16 1st	Sin Wave 1st Mode	
		C16 2nd	Sin Wave 2nd Mode	
		C16 E once	1940 El Centro EW	
		C16 E 1/8	"	1/8 Time Scale
	Isolated Wall	IS16 E	"	
		IS16 T	1952 Taft S69E	
		IS16 1st	Sin Wave 1st Mode	
		IS16 2nd	Sin wave 2nd Mode	
		IS16 Eonce	1940 El Centro EW	
	Center Core Structure	C16 pt E	"	pt*2 normal pt
		C16 pw E	"	pw*1/4 normal pw

Table 2 Material Properties

		Strength (kg/cm²)	Young Modulus (x10⁵ kg/cm²)
concrete		357.	2.21
steel	3.2φ	3500.	21.00
	1.0φ	3100.	21.00

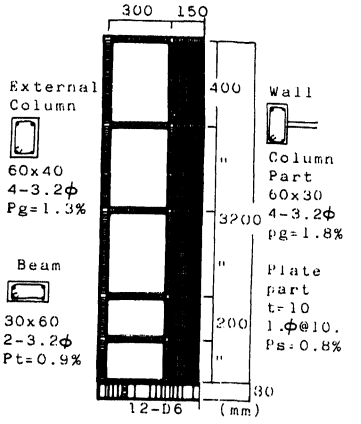

Fig. 1 Details of Test Structure

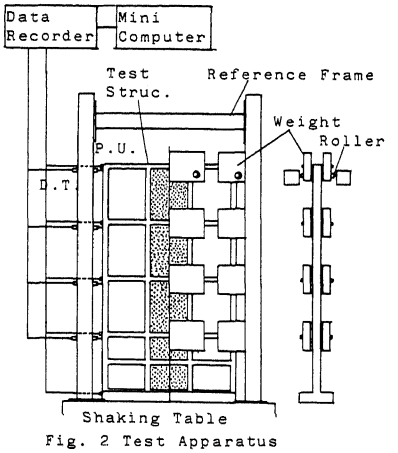

Fig. 2 Test Apparatus

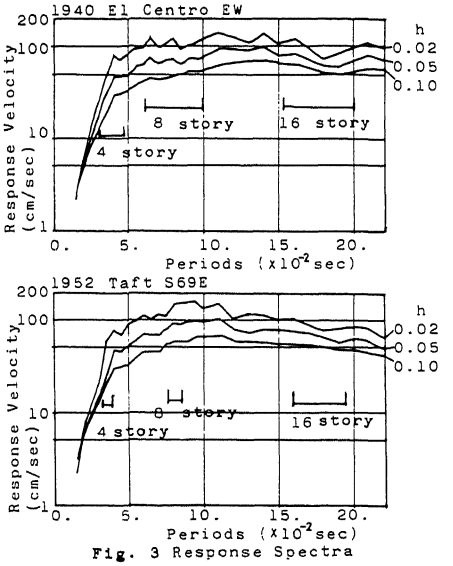

Fig. 3 Response Spectra

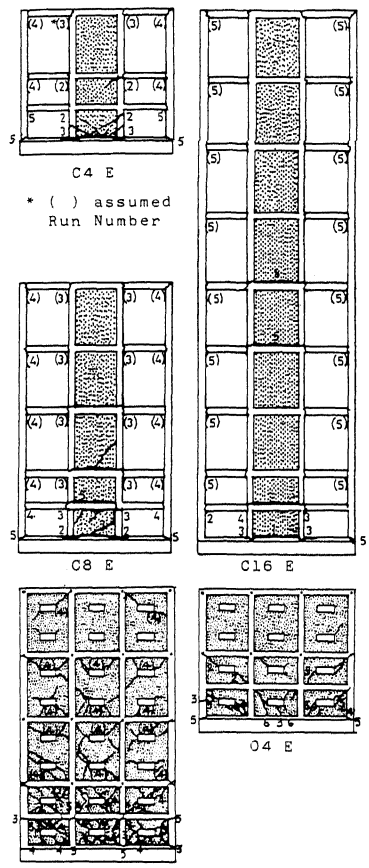

Fig. 4 Crack Patterns

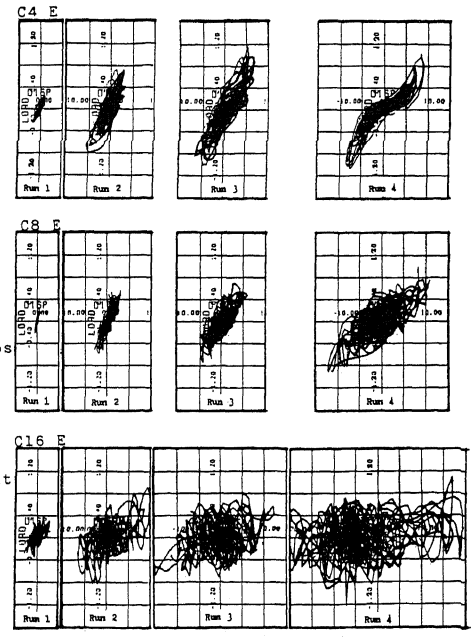

Fig. 5
Hysteresis loops

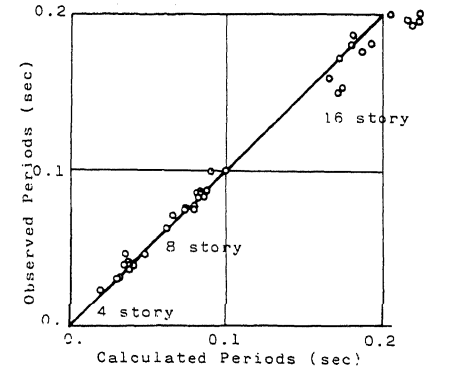

Fig. 7 Initial Fundamental Periods

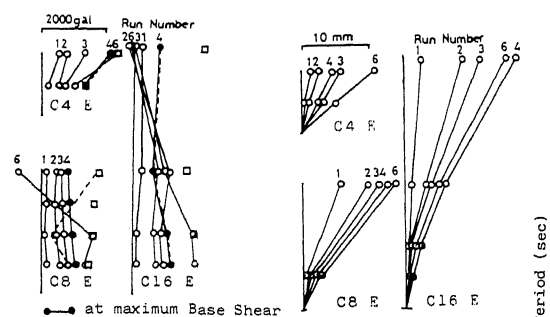

Fig. 6-a
Lateral Load Distribution Shape at Maximum Base Shear in Each Run

Fig. 6-b
Lateral Disp. Distribution Shape at Maximum Top Floor Disp. in Each Run

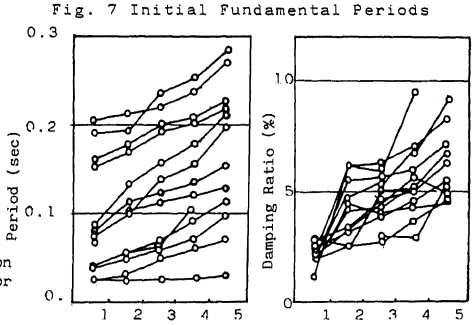

Fig. 8 Increasin Periods and Equivalent Damping Ratios with Input Levels

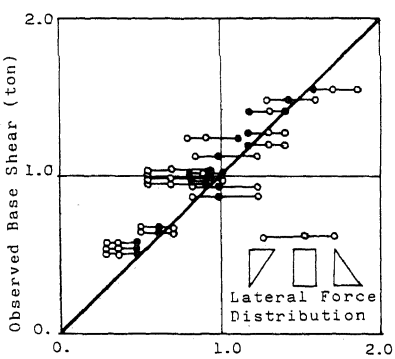

Fig. 9 Maximum Base Shear

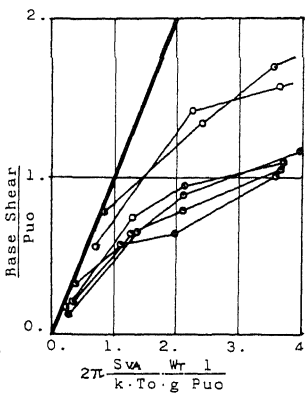

Fig. 10 Observed maximum Base Shear versus Calculated Values Obtained from Eq. (1-a)

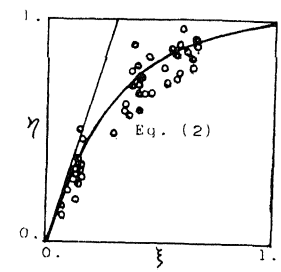

Fig. 11
Normalized Curve Obtained from Fig. 6 with Respect to Each Maximum Values in Both the Coordinates

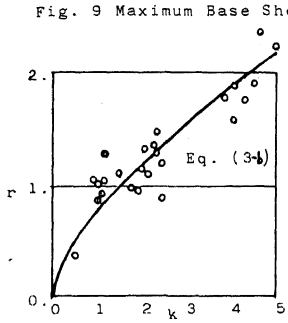

Fig. 12
Ratios of Observed Base Shear to Ultimate Strength Calculated by Assuming Inverted Triangular Distribution for Lateral Loads

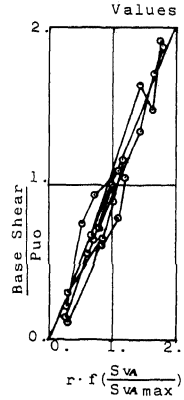

Fig. 13 Maximum Base Shear versus Calculated Values Obtained from Eq. (4-a)

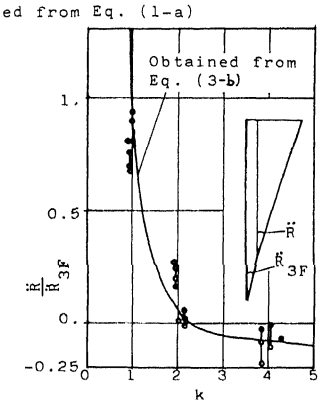

Fig. 14
Ratios of Relative Accelerations between Top and Third Floor to Ones at Third Floor

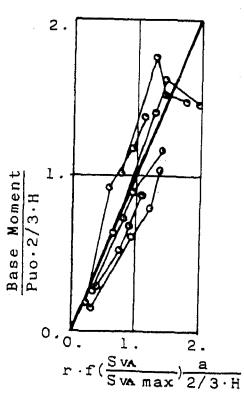

a=2.27 for 16 story
a=1.20 for 8 story
a=0.67 for 4 story

Fig. 15
Observed Base moment versus Calculated Values

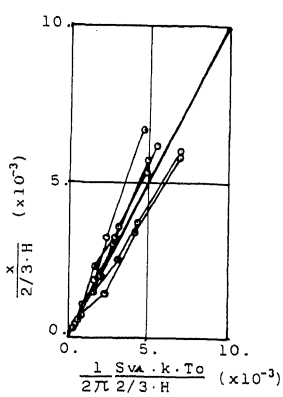

Fig. 16
Observed Maximum Deformation Angle versus Calculated Values Obtained from Eq. (5)

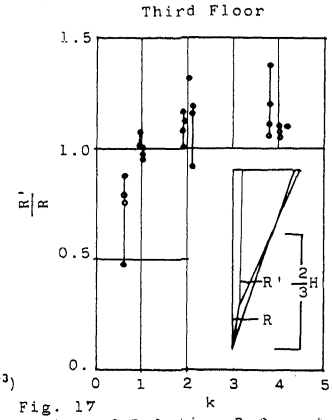

Fig. 17
Ratios of Relative Deformation Angle between Top and Third Floors to Average Deformation angle at the Height of 2/3 H

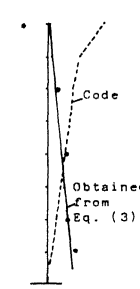

Fig. 18
Comparison between Eq.(3) and Code for sixteen story